

Punctuated equilibrium and “history-dependent” percolation

Božidar Jovanović,¹ Sergey V. Buldyrev,¹ Shlomo Havlin,^{1,2} and H. Eugene Stanley¹

¹Center for Polymer Studies and Department of Physics, Boston University, Boston, Massachusetts 02215

²Department of Physics, Bar-Ilan University, Ramat Gan, Israel

(Received 7 April 1994)

We study the Bak-Sneppen (BS) punctuated equilibrium model of biological evolution and calculate its critical exponents. We show that this model can be mapped onto a two-dimensional model of the invasion percolation type, which is “history dependent,” in that the exponents depend on the *order* in which the sites of the system are updated. We find that the critical exponents γ , ν_{\perp} , σ , and ω for the BS model are different from those of the directed percolation model, but the combination $\sigma\nu_{\perp}$ is the same.

PACS number(s): 05.40.+j, 87.10.+e

I. INTRODUCTION

Some 20 years ago, Gould and Eldredge introduced a theory of punctuated equilibrium of ecological systems in order to explain the phenomenon of biological evolution [1]. This theory states that the evolution takes place in terms of sudden outbursts of activity, which are separated by long periods of stability. It has been suggested that for this reason ecological systems evolve into a self-organized critical (SOC) state [2].

Bak and Sneppen (BS) have recently proposed a SOC model for punctuated equilibrium [3]. It has an important advantage over previous models, because it does not need an external tuning parameter to evolve into the critical state [4]. In the BS model, every species is represented by a single parameter, called the “fitness.” The fitness parameter can be regarded as a complex combination of factors such as genetic material and forces of natural habitat. The interaction between species and the dynamics in the model is introduced by assuming the fitness of each species is affected by the fitnesses of the species surrounding it. Species adapt into a rugged multi-peaked fitness landscape. The system usually “finds” a local fitness maximum very fast, and remains there. However, the scaling properties of the BS model and its relation to known statistical models such as percolation remains unclear.

We propose here a “history-dependent” invasion percolation type model, and we study three types of updating rules (models 1–3). Model 1 will be mapped to the BS model, while models 2 and 3 yield different exponents. A similar mapping was presented recently in [5], where the idea of relating to directed percolation is originally proposed.

II. “HISTORY-DEPENDENT” PERCOLATION MODELS

We begin with a square lattice, each cell of which is characterized by its fitness p_i , which is a random number between 0 and 1, Fig. 1. We describe the history-dependent percolation models using the language of fluid imbibition [6,7].

Assume that at $t=0$, the interface is horizontal. All cells with a coordinate $y < 0$ are wet, while all cells with $y \geq 0$ are dry. Each vertical column of the system represents a species where the values of the fitnesses of the cells with $y=0,1,2,\dots$ represent the subsequent values of fitnesses

that this species will acquire in the process of evolution. The current value of fitness of a particular species is defined by the fitness of the lowest dry cell in its column.

At each three subsequent time steps ($t, t+1, t+2$), the liquid propagates by one cell in three neighboring columns. The order in which the three cells are occupied is random. The central column must have fitness below a certain preassigned value p . The fitness values of the side columns are irrelevant. If there is more than one column with fitness less than p , we select the central column according to a specific model-dependent rule (see below).

At steps $t+3, t+4, t+5$, we use the same rule to select three new columns. This process corresponds to a mutation of the species represented by the central column and a con-

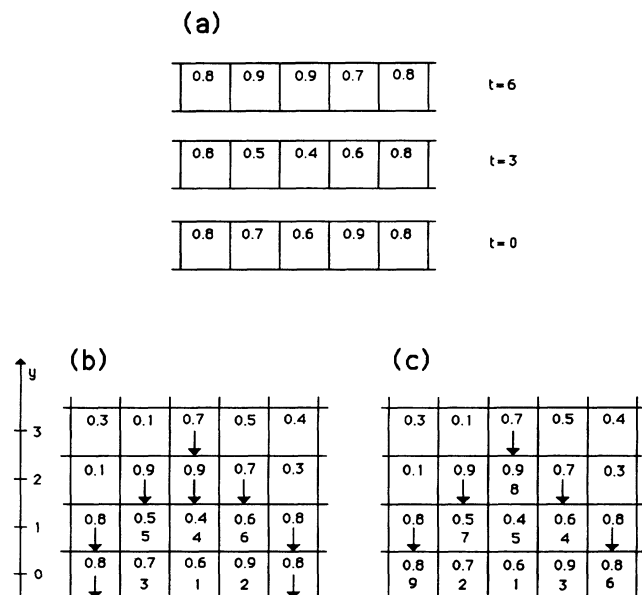


FIG. 1. (a) Three updating steps of the BS model. (b) Model 1 represents a two-dimensional mapping of the BS model. (c) Model 2 is a variant of two-dimensional percolation with a different updating order. The top number of each cell is the fitness p_i . The bottom number in (b) and (c) is the order of updating. In (c), the numbers in the cells represent the fitness of the species at time t . The arrows in the cases (b) and (c) point to the cells that cannot be chosen as central because $p_i > p$, where $p = 0.66$ here.

sequent change of the fitnesses of its neighbors. The process is iterated until the fitness value of all columns is above p . This corresponds to an avalanche of mutations specified by the value of p .

We investigate three models which differ by a rule of how the position of the central column is selected.

Model 1. The column with the smallest fitness value is selected [see Fig. 1(b)].

Model 2. The last updated column with fitness smaller than p is selected [see Fig. 1(c)].

Model 3. The column for updating is selected randomly among those with fitnesses smaller than p .

Figure 1(a) represents the evolution of the one-dimensional BS model. In our example, we have an avalanche of size 6. If we place the one-dimensional arrays, representing the successive time steps of the BS model, on the square lattice, we can see that the geometrical properties of this avalanche are exactly the same as for model 1, represented in Fig. 1(b). In both models, there exists a critical parameter $p = p_c$ below which the avalanches are finite, but above which there is a finite probability to obtain an infinite avalanche. If we choose $p > p_c$, then the behavior of the infinite system described by model 1 is exactly the same as for the BS model. For $p < p_c$, the behavior described by model 1 is the same as in the BS model within the single avalanche defined by the value p at which the avalanche has started.

This mapping shows that the one-dimensional BS model has the same avalanches and therefore the same critical behavior as model 1 for dimension $d = 2$. However, it is clear from Figs. 1(b) and 1(c) that even for the same configurations of the lattice disorder, the avalanches for models 1 and 2 are quite different. Our numerical simulations suggest that models 1 and 2, which differ only in their updating order, are in different universality classes. This finding is in contrast to the regular percolation models such as directed percolation (DP) or invasion percolation, for which the shapes of the clusters are independent of the growth history [8].

III. RESULTS

Our results are obtained by computer simulations of systems of linear size $L = 2^{14} = 16384$. Averages are taken over 10^5 configurations. We study the following quantities by assuming their scaling forms in analogy with percolation [8].

(1) The number of avalanches of size s behaves as

$$n(s) \sim s^{-\tau} f(s|p - p_c|^{1/\sigma}), \quad (1)$$

when approaching p_c (see Fig. 3).

(2) The number of avalanches with horizontal base of length b is

$$n(b) \sim b^{-\tau_\perp} f(b|p - p_c|^{\nu_\perp}). \quad (2)$$

From the relation $n(b)db = n(s)ds$, we find

$$\tau_\perp - 1 = \frac{\tau - 1}{\nu_\perp \sigma}. \quad (3)$$

The quantity $\sigma \nu_\perp$ describes how a typical avalanche of base b scales with typical cluster size s . In our models, s is exactly equal to the number of steps, or time t , so

$$b(t) \sim t^{\sigma \nu_\perp}. \quad (4)$$

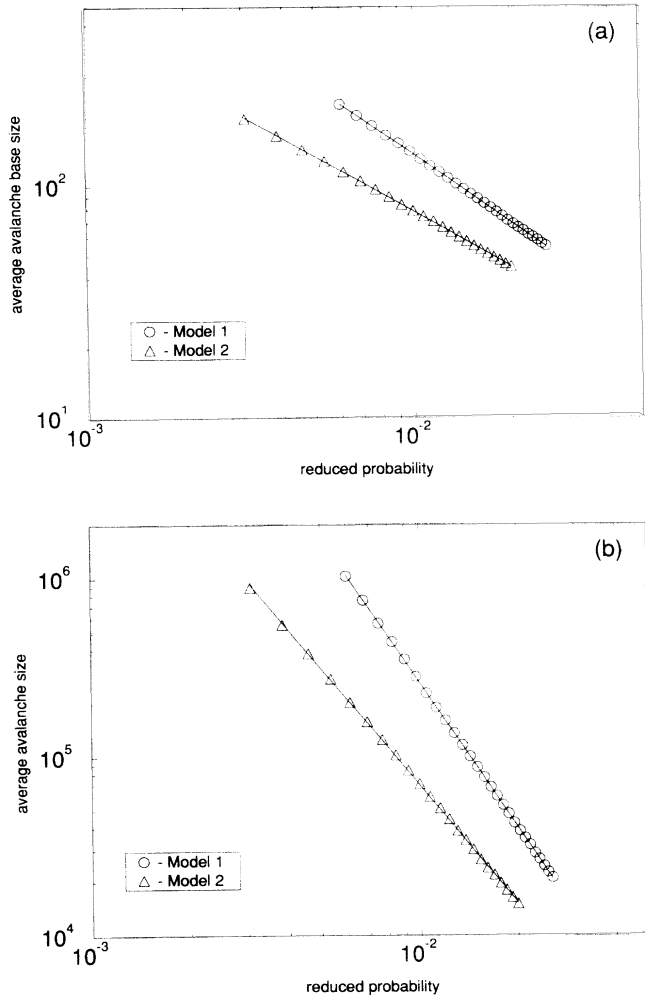


FIG. 2. (a) The mean horizontal size of the avalanche $\langle b \rangle$ is plotted as a function of reduced probability $[(p_c - p)/p_c]$ for models 1 and 2, on a log-log plot. (b) The average avalanche size $\langle s \rangle$ as a function of reduced probability $[(p_c - p)/p_c]$ for models 1 and 2, on a log-log plot. The exponents γ_\perp and γ are different for models 1 and 2. The value of p_c was obtained by the best linear fit of the data points.

(3) The mean avalanche size $\langle s \rangle \sim |p - p_c|^{-\gamma}$ [see Fig. 2(b)].

(4) The mean horizontal length of the base of the avalanche

$$\langle b \rangle \sim |p - p_c|^{-\gamma_\perp} \quad (5)$$

where $\gamma_\perp = \nu_\perp - \beta$ [8] [see Fig. 2(a)].

(5) Diffusion of mutations. Following BS, we study the coordinate $x(t)$ of the site that we update at time t , and the distribution $P(\Delta x)$ of distances $\Delta x = x(t) - x(t-1)$ between the successive updates. We find

$$P(\Delta x) \sim |\Delta x|^{-\omega}. \quad (6)$$

The function $x(t)$ visually resembles a random walk with a power law distribution of step length. Such a random walk with uncorrelated steps is known as a Lévy flight [9]. It is known that for $\omega > 3$, the mean square displacement of the

TABLE I. Results for models 1–3 and directed percolation.

	Model 1	Model 2	Model 3	Directed percolation
p_c	0.667 ± 0.001	0.653 ± 0.001	0.635 ± 0.001	0.645
γ	2.7 ± 0.1	2.2 ± 0.1	2.3 ± 0.1	2.28
τ	1.08 ± 0.05	1.08 ± 0.05	1.08 ± 0.05	1.12
σ	0.35 ± 0.02	0.40 ± 0.02	0.40 ± 0.02	0.39
ω	3.1 ± 0.2	3.2 ± 0.2	N/A	2.1 ± 0.2
γ_{\perp}	0.98 ± 0.03	0.80 ± 0.02	0.83 ± 0.02	0.82
ν_{\perp}	1.23 ± 0.08	1.07 ± 0.08	1.11 ± 0.08	1.097
ν_{\parallel}	1.8 ± 0.1	1.4 ± 0.1	1.4 ± 0.1	1.73
γ/γ_{\perp}	2.75 ± 0.08	2.75 ± 0.08	2.75 ± 0.08	2.78
$\sigma\gamma$	0.92 ± 0.05	0.89 ± 0.05	0.92 ± 0.05	0.89
$\sigma\nu_{\perp}$	0.43 ± 0.01	0.43 ± 0.01	0.43 ± 0.01	0.43

Lévy flight $\langle x^2 \rangle \sim t$, as for the regular random walk. In our case, however, $\langle x^2 \rangle$ scales with time exactly the same way as the horizontal size of the avalanche scales with its mass s [see Eq. (4)]. Thus the quantity $\sigma\nu_{\perp}$ can be considered as the diffusion exponent. We measured $\sigma\nu_{\perp}$ using Eqs. (4) and $\langle x^2 \rangle \sim t^{2\sigma\nu_{\perp}}$, and we found excellent agreement between the results obtained by these two methods.

Using our calculations of $\langle s \rangle$ and $\langle b \rangle$, we calculated the critical probability p_c and critical exponents γ_{\perp} and γ for models 1–3. The results are presented in Table I. All the exponents and combinations of exponents have been measured numerically, except $\sigma\gamma$ which was obtained by multiplication. In order to compare our models with the model of DP we include in the table the known exponents for DP [8]. The exponent ω is not defined in the classical DP problem, however, it can be defined for an invasion directed percolation where the next site to be included in the cluster is selected as the site with the smallest value of pinning force. The growth activity of such clusters jumps from one site to the next, similar to the way it jumps in the BS model. We have studied the invasion directed percolation numerically and find that the components of these jumps perpendicular to the direction of growth are distributed according to Eq. (6). The exponent ω of this distribution is reported in Table I. The value of the percolation threshold p_c for the DP model reported in Table I is the value for bond directed percolation on the square lattice [8]. The values of the thresholds for other types of DP can be significantly different [10]. The error bars have been tested by applying our method to the DP model, for which accurate values of exponents are known.

IV. DISCUSSION

The results in Table I and Figs. 2 and 3 suggest that models 1 and 2 are in different universality classes. The difference in the critical exponent γ between the two models is much larger than the error bars. The exponents of model 2, with the exception of the exponent ω and γ_{\perp} , are very close to the exponents of directed percolation. However, the quality of our data is not sufficient to claim that they are exactly the same.

In contrast with the exponents characterizing the scaling of the variables with $|p-p_c|$ (such as γ and ν_{\perp}), the com-

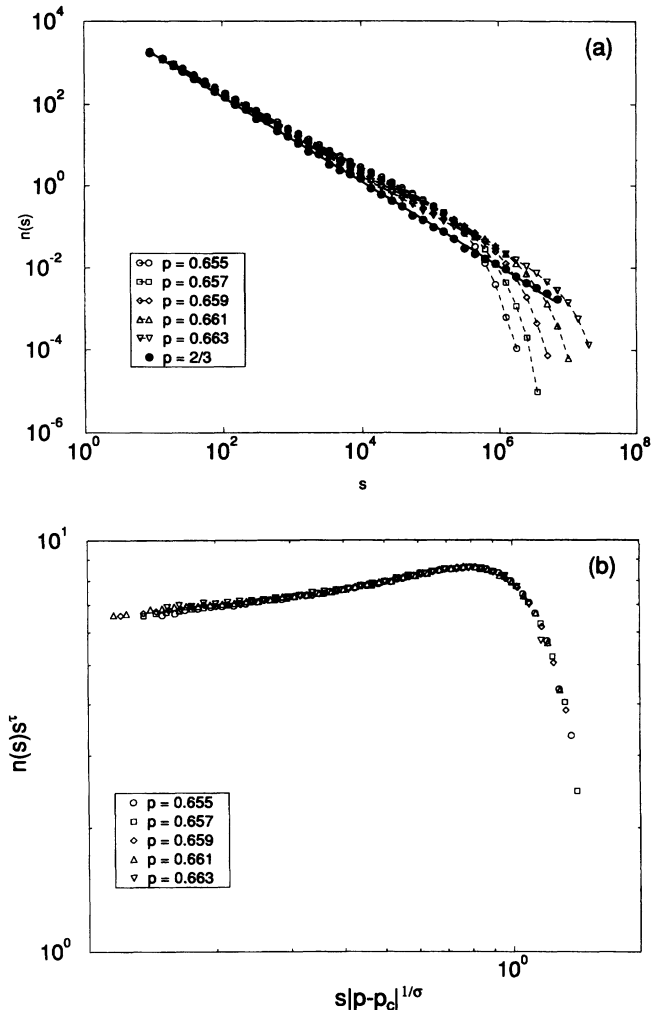


FIG. 3. (a) The distribution of avalanches $n(s)$ as a function of s , on a log-log plot for model 1. The points with dashed lines are for different simulations with $p < p_c$, while the straight line is the best linear fit of the data for $p = p_c$. (b) Shows the data collapse for $p < p_c$.

binations of these exponents which characterize relations between the variables describing purely geometrical properties of the avalanches (such as the diffusion exponent $\sigma\nu_{\perp}$) are very close for all three models. A similar observation was made by Prakash *et al.* [11], while studying percolation models with long-range correlations. This may indicate the existence of *superuniversality*, which would be broader than the standard universality. The models for which the combinations of critical exponents are equal would be in the same superuniversality class, although they may not be in the same class with respect to the standard exponents. Therefore we suggest that the “superuniversality class” of directed percolation includes the BS model, models 1–3, as well as several other models such as ballistic deposition with poisoned sites.

The dependence of exponent ω on the dynamics of the process suggests that this is an independent dynamical exponent, which cannot be simply related to classical exponents, such as σ and τ .

It is interesting to note that in contrast with directed per-

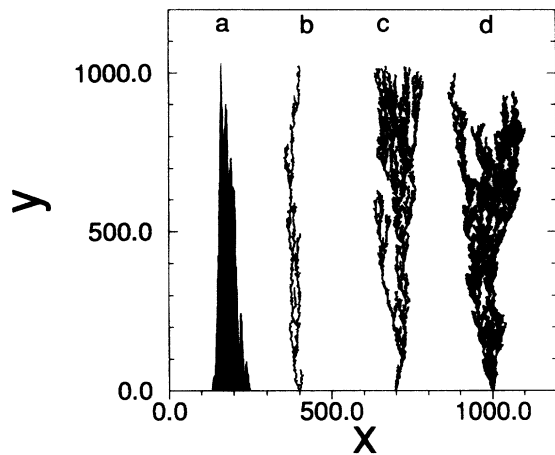


FIG. 4. The shapes of clusters for (a) model 1, (b) ballistic deposition variant of model 1, (c) ballistic deposition variant of model 3, and (d) invasion directed percolation. Each is presented when the height reaches 1000 lattice units.

colation, models 1–3 produce geometrically compact avalanches [see Fig. 4(a)], for which (see also [10])

$$\nu_{\perp} + \nu_{\parallel} = 1/\sigma = \gamma + \beta. \quad (7)$$

However, models 1–3 can be modified in such a way that the heights of all three updated columns in three subsequent time steps are taken to be equal to the highest of the three. Such models can be described as variants of *ballistic deposition* of rectangular bricks of width 3 and height 1. These models produce ramified avalanches similar to one shown on Figs. 4(b,c), which is the reason why Eq. (7) does not hold for them. All the exponents of these modifications are the same as for corresponding models 1–3 except ν_{\parallel} . We calculated

the values of ν_{\parallel} , and found that for modified model 1 $\nu_{\parallel}/\nu_{\perp} = 2.1 \pm 0.1$ and for modified model 2 $\nu_{\parallel}/\nu_{\perp} = 2.3 \pm 0.1$, indicating that the avalanches of modified models 1 and 2 are more elongated than the clusters of DP [see Fig. 4(d)], for which $\nu_{\parallel}/\nu_{\perp} = 1.58$. However, for modified model 3 we get $\nu_{\parallel}/\nu_{\perp} = 1.6 \pm 0.1$. Indeed, clusters for modified model 3 look very similar to the DP clusters [see Fig. 4(d)]. The hyperscaling relation

$$\nu_{\perp} + \nu_{\parallel} = 1/\sigma + \beta = \gamma + 2\beta \quad (8)$$

is valid for DP, but is violated by models 1 and 2 proposed here, and is probably correct for the ballistic deposition variant of model 3.

The similarities between certain combinations of exponents such as the diffusion exponent $\sigma\nu_{\perp}$, observed in Ref. [5] and our work, may indicate the existence of a *superuniversality* class that includes both BS and DP models. However, the striking differences between models 1 and 2, and the DP model, as well as their unusual dependence on the history of growth, do not support the recent argument [5] that the BS model is in the universality class of Reggeon field theory, which is known to be represented by the DP model. Exponents $\gamma, \sigma, \omega, \nu_{\perp}$ are different for model 1 (which is the same as BS) and for DP, therefore suggesting that they belong to different universality classes. This claim is supported by the avalanche shape analysis done above.

After this work was completed we learned that the observation that the original BS model is in its essence two-dimensional was made independently by Ray and Jan [12].

ACKNOWLEDGMENTS

The authors would like to thank Professor Naeem Jan for very helpful discussions. The Center for Polymer Studies is supported by the NSF.

-
- [1] S. J. Gould and N. Eldredge, *Nature (London)* **366**, 223 (1993).
 [2] P. Bak, K. Chen, and M. Creutz, *Nature (London)* **342**, 780 (1989).
 [3] P. Bak and K. Sneppen, *Phys. Rev. Lett.* **71**, 4083 (1993).
 [4] S. A. Kauffman and S. J. Johnsen, *J. Theor. Biol.* **149**, 467 (1989).
 [5] M. Paczuski, S. Maslov, and P. Bak, Brookhaven National Laboratory Report No. BNL-49916, 1993 (unpublished); *Europhys. Lett.* **27**, 96 (1994).
 [6] T. Vicsek, *Fractal Growth Phenomena*, 2nd ed. (World Scientific, Singapore, 1992).
 [7] L.-H. Tang and H. Leschhorn, *Phys. Rev. A* **45**, R8309 (1992); S. V. Buldyrev, A.-L. Barabási, F. Caserta, S. Havlin, H. E. Stanley, and T. Vicsek, *ibid.* **45**, R8313 (1992); S. Havlin, A.-L. Barabási, S. V. Buldyrev, C. K. Peng, M. Schwartz, H. E. Stanley, and T. Vicsek, in *Growth Patterns in Physical Sciences and Biology*, Proceedings of the NATO Advanced Research Workshop, Granada, Spain, 1991, edited by J. M. Garcia-Ruiz, E. Louis, L. Sander, and P. Meakin (Plenum, New York, 1993).
 [8] *Fractals and Disordered Systems*, edited by A. Bunde and S. Havlin (Springer, Heidelberg, 1991), Chaps. 2 and 3; J. Kertesz and T. Vicsek, in *Fractals in Science*, edited by A. Bunde and S. Havlin (Springer, Berlin, 1994); A.-L. Barabási and H. E. Stanley, *Fractal Concepts in Surface Growth* (Cambridge University Press, Cambridge, 1995); A.-L. Barabási, S. V. Buldyrev, S. Havlin, G. Huber, H. E. Stanley, and T. Vicsek, in *Surface Disordering: Growth, Roughening, and Phase Transitions*, edited by R. Jullien *et al.* (Nova Science, New York, 1992).
 [9] M. F. Shlesinger, G. M. Zaslavsky, and J. Klafter, *Nature (London)* **363**, 31 (1993).
 [10] S. V. Buldyrev, S. Havlin, and H. E. Stanley, *Physica A* **200**, 200 (1993).
 [11] S. Prakash, S. Havlin, M. Schwartz, and H. E. Stanley, *Phys. Rev. A* **46**, R1724 (1992).
 [12] T. Ray and N. Jan, *Phys. Rev. Lett.* **72**, 4045 (1994).